



Agent-Based Models for Collective Animal Movement: Proximity-Induced State Switching

Authors: Andrew Hoegh, Frank T. van Manen, and Mark Haroldson

The final publication is available at Springer via <https://doi.org/10.1007/s13253-021-00456-0>

Hoegh, A., van Manen, F.T. & Haroldson, M. Agent-Based Models for Collective Animal Movement: Proximity-Induced State Switching. *Journal of Agricultural, Biological and Environmental Statistics* (2021). <https://doi.org/10.1007/s13253-021-00456-0>

Made available through Montana State University's [ScholarWorks](https://scholarworks.montana.edu)
scholarworks.montana.edu

Agent-Based Models for Collective Animal Movement: Proximity-Induced State Switching

May 26, 2021

Abstract

Animal movement is a complex phenomenon where individual movement patterns can be influenced by a variety of factors including the animal's current activity, available terrain and habitat, and locations of other animals. Motivated by modeling grizzly bear movement in the Greater Yellowstone Ecosystem, this article presents an agent-based model represented in a state-space framework for collective animal movement. The novel contribution of this work is a collective animal movement model that captures interactions between animals that can trigger changes in movement patterns, such as when a dominant grizzly bear may cause another subordinate bear to temporarily leave an area. The modeling framework enables learning different movement patterns through a state-space representation with Particle-MCMC methods for fully Bayesian model fitting and the prediction of future animal movement behaviors.

Keywords: Bayesian statistics, MCMC, Particle-MCMC

1 Introduction

Animal movement is a complex phenomenon driven by a variety of factors including interactions with other animals. However, until recently, most statistical models for animal movement did not consider interactions among individual animals. Collective animal movement models, where individual animals interact and influence each other, present a challenge. Part of the challenge is the model specification, which can require complicated non-linear interactions between individuals, whereas the other part is computational, in that jointly considering the simultaneous position of all animals prevents parallel computation and can require evaluating complicated non-linear interactions among individuals.

A variety of approaches are used for animal movement models: one foundation is based on velocity between consecutive measurement fixes (Jonsen et al., 2005), which is often constructed using step length and turning angles. The simplest of these animal movement models use correlated or biased random walks, where the animal’s directional heading depends on previous angle or is biased toward a location or direction. Habitat or terrain can influence animal movement, hence, these can also be incorporated into animal movement models (Christ et al., 2008; Peck et al., 2017). For a comprehensive overview of animal movement modeling, readers are referred to Hooten et al. (2017).

More complex animal movement patterns can also be included, such as those that depend on the animal’s behavioral state (e.g., exploring or foraging). Langrock et al. (2012) provides an overview of hidden Markov models for discrete time, which enable different turning angles and step lengths for a set of animal states. State switching models can also be useful as an animal can have different movement patterns corresponding to different behavioral states. Morales et al. (2004), Haydon et al. (2008), and McClintock et al. (2012) present frameworks for multistate models that account for different behavioral states. In a related setting, Scharf et al. (2019) models polar bear movement and incorporates a dynamic covariate response to correspond to changing resources, allowing behavior to change as resources change.

Collective animal movement models require jointly evaluating positions of all animals in a

28 study area; although, models have been implemented in different ways. In the ecology litera-
29 ture, rule-based methods are common. Couzin et al. (2002) presents a rule-based framework
30 based on animals minimizing the distance between each individual coupled with a zone of
31 repulsion. These models can capture many different collective dynamics including swarming
32 behavior often exhibited in insects or parallel groups often exhibited by flocks of birds or
33 schools of fish. Couzin et al. (2005) also presents a framework that allows groups of animals
34 to make collective movement decisions based on social interaction within the group. Bal-
35 lerini et al. (2008) summarizes rule-based ecological collective movement models by stating,
36 "...the models agree on three general behavioral rules: move in the same direction as your
37 neighbours; remain close to them; avoid collisions." While ecological models for collective
38 movement tend to be rule-based, statistical frameworks for animal movement are generally
39 model-based which enable learning model parameters directly from observed collective move-
40 ment datasets and can be used to generate k-step ahead predictions given current animal
41 locations. Langrock et al. (2014) uses correlated and biased random walks to develop a col-
42 lective animal movement model, where animals are attracted to the moving centroid of the
43 group. In addition to attraction to the groups centroid, Langrock et al. (2014)'s framework
44 also incorporates a state that permits the animal to explore independently of the group by
45 temporarily removing or reducing the attraction to the group centroid. Agent-Based Models
46 (ABMs) are another approach for collective animal movement that have gained popularity
47 in the last decade (Hooten and Wikle, 2010; Bonnell et al., 2016; McDermott et al., 2017).

48 A major benefit of ABMs for animal movement is that complicated interactions between
49 individuals can be modeled in a relatively simple manner. ABMs provide a simulation
50 approach built on behaviors of a group of *agents*. The agents interact with each other based
51 on a set of rules to provide a mechanism for modeling individual-level behavior, but the
52 collective response of the agents can be used to understand population-level characteristics.
53 Individual agents can be calibrated with fairly simple behaviors; but the collective response
54 of the agents can model complex population dynamics. While ABMs have been used in

55 many situations (for instance, Gilbert and Terna (2000); Brown et al. (2005); Gilbert (2008);
56 Farmer and Foley (2009)), statistical parameter estimation with uncertainty is fairly new,
57 particularly in an animal movement framework.

58 One challenge with ABMs from a statistical perspective has been capturing the uncer-
59 tainty in parameter estimation. The individual dynamics and nonlinear functions that result
60 from a set of behavioral rules for agents can make evaluating likelihoods, and thus many
61 likelihood-based or Bayesian approaches, difficult or impossible. One recent approach (Mc-
62 Dermott et al., 2017) for ABMs with animal movement models used Approximate Bayesian
63 Computation (ABC) (Beaumont et al., 2002; Beaumont, 2010) for model fitting. In addi-
64 tion to ABC approaches, Particle-MCMC (P-MCMC) methods (Andrieu et al., 2010) are
65 also recommended for model fitting with nonlinear state space models (Fasiolo et al., 2016);
66 however, we are not aware of their use in ABMs for collective animal movement.

67 The motivating research goal for this work is to calibrate an ABM to capture the col-
68 lective dynamics of grizzly bear (*Ursus arctos*) movement with a focus on long term land
69 use patterns. With collective grizzly bear movements and the associated ABMs, there are
70 several features that inform model choice, which is specified through the agent rules. The
71 collective behavior of grizzly bears is fundamentally different than schooling behavior mod-
72 eled with a self-propelled particle (Vicsek et al., 1995) as formulated in McDermott et al.
73 (2017) or the herd-like behavior in Langrock et al. (2014), and thus, requires a new model
74 formulation. Dominance hierarchies in grizzly bears can induce repulsive forces; however,
75 there may also be times when bears are attracted to each other: during breeding season, for
76 family dynamics, or when there is a local abundance of food resources. Hence, models of
77 collective behavior should allow for both attractive and repulsive forces. Furthermore, the
78 models can include hierarchical treatment of movement patterns that allow each individual
79 bear to have its own movement parameters. In addition to specifying an ABM for collective
80 grizzly bear movement, another novel contribution of this modeling framework is the inclu-
81 sion of a Markov switching component where changes in behavioral states can be influenced

82 by other bears.

83 This article extends existing ABMs for animal movement models through the lens of
84 state-space models and introduces P-MCMC methods for computing those models. Whereas
85 the application focuses on grizzly bears in the Greater Yellowstone Ecosystem (GYE), the
86 methods are applicable to a range of species and contexts. In Section 2 we describe the
87 structure of the data, Section 3 provides an overview of our ABM modeling framework for
88 grizzly bears, Section 4 details computation for fitting these models, Section 5 provides a
89 set of simulation studies and an analysis of grizzly bear movement data in the GYE, and
90 Section 6 concludes with a discussion.

91 **2 Data Overview**

92 The dataset used for this analysis contains telemetric GPS locations of 91 male grizzly bears
93 in the GYE from 2005 – 2015. Captures were conducted under U.S. Fish and Wildlife
94 Service Endangered Species Permit [Section (i) C and D of the grizzly bear 4(d) rule, 50
95 CFR17.40(b)], with additional permits from the National Park Service, Wyoming, Montana,
96 and Idaho, and conformed to the Animal Welfare Act and to U.S. Government principles
97 for the use and care of vertebrate animals used in testing, research, and training (USGS
98 ACUC no. 201201). The bears are instrumented with telemetric tracking devices that record
99 consecutive location fixes. Given the crepuscular behavioral patterns that bears exhibit, the
100 location fixes are filtered to include one data point from the morning twilight hours and one
101 from evening twilight hours. In particular, the location fixes nearest to 7:30 AM and PM on
102 each day are retained for the analysis. This corresponds to time periods when bears are most
103 active and hence, most likely to interact with other animals. Models are fit using data from
104 May through August and predictions are made for September of each year. Data are recorded
105 until the tracking devices failed, were shed as scheduled using pre-set drop-off mechanisms,
106 or were removed during recaptures. Some of bears were recaptured and collared at a later

107 date, so it is possible to have location fixes that are separated by many years. Bears without
108 a minimum of 20, twice-daily consecutive location fixes are removed from the dataset.

109 Grizzly bear locations, and animal movement in general, are best visualized with ani-
110 mation, such as using the anipaths package in R (Scharf, 2019); however, Figure 1 contains
111 static summaries of grizzly bear locations created in R with packages from Pedersen (2019),
112 Wickham (2016), and Kahle and Wickham (2013). Figure 1 contains telemetric locations of
113 bears observed in 2014 and 2015. Each bear in a given year is represented in a different color
114 and locations are bounded with a convex hull to capture an approximate home range.

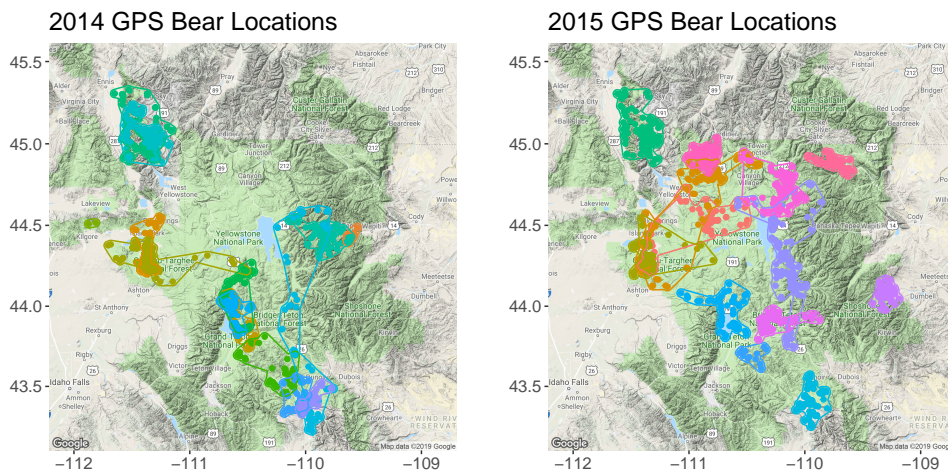


Figure 1: Locations of male grizzly bears during 2014 - 2015. While there are similar shades of colors, the same color across both years indicates a bear with GPS location data for both years. The outlines represent approximate range of each bear, constructed with a convex hull.

115 Past research has shown that different behavioral states can be inferred from telemet-
116 ric movement patterns (Ebinger et al., 2016). For instance, when bears are exploring and
117 searching for new territory the step size will tend to be larger and the turning angles, between
118 consecutive fixes, will be smaller. In other words, the bears tend to move in the same heading
119 for an extended time. This can be seen in Figure 2, which displays the turning angle as a
120 function of step size to illustrate differences associated with smaller versus larger movement
121 steps. With the smaller steps, bears tend to have a more uniform turning angle, with addi-

122 tional mass near 180 degree turns that would correspond to returning to a previous location.
123 With larger step size, bears tend to maintain an existing heading, as a large proportion of
124 the turning angles reside within 60 degrees of 0. These longer, directed movements are often
125 associated with attracting or repulsive forces (e.g., mating, avoidance of dominant animals
126 or areas of high density, dispersal) or shifts in resource use.

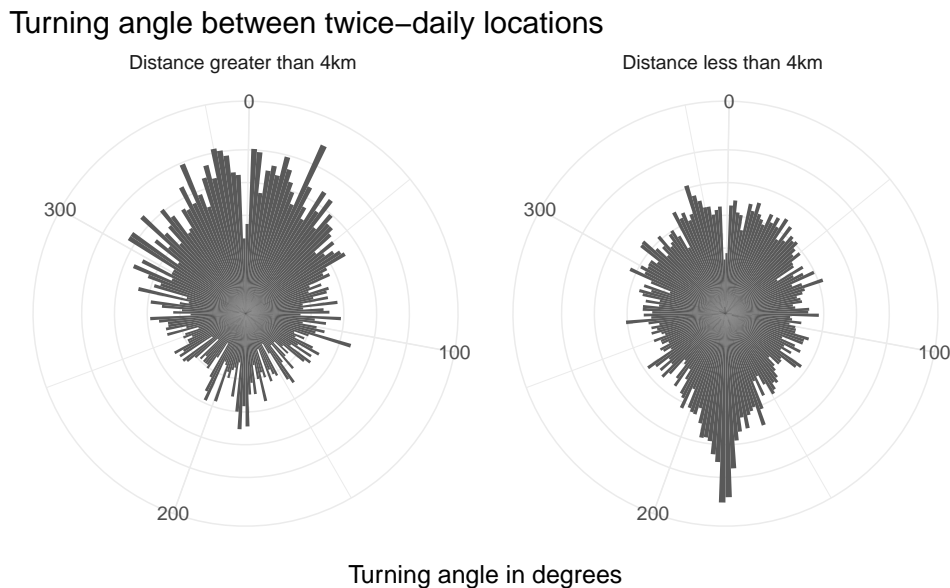


Figure 2: Turning angles associated with step sizes less than or greater than 4 kilometers. The longer step sizes tend to maintain the previous heading, while the shorter step sizes tend to have a more uniform distribution, with a large number of movement patterns around 180 degrees, which would correspond to returning to a previous location. A distance of 4 kilometers represents about the 80th percentile of step sizes, but the figure is fairly robust to changes in the percentile value.

127 **3 Modeling Framework**

128 The main contribution of this article is to formalize a state-space framework for ABMs with
129 collective animal movement focusing on species that do not exhibit schooling or herd-like
130 behavior. The article also details particle methods for fully Bayesian computation. The

131 modeling framework enables collective animal movement models that incorporate attractive-
 132 repulsive forces in a behavioral switching model along with a hierarchical model structure.

133 **3.1 Model Specification**

134 Building on the ABM model specification in McDermott et al. (2017), we describe our
 135 model through a state-space framework and add additional features necessary to capture
 136 the complex dynamics that drive grizzly bear movement. Given the applicability for general
 137 animal movement models, the model specification is explained in general terms using agents
 138 in place of bears.

139 **Observation Equation**

The observation equation is specified using model notation from McDermott et al. (2017). Assume that spatial locations of the $i = 1, \dots, N$ agents are obtained at discrete times, $t = 1, \dots, T$. Then the observed locations at time t are defined as $\mathbf{z}_t \equiv \{\mathbf{z}'_{i,t}\}_{i \in 1, \dots, m_t}$, where $\mathbf{z}'_{i,t} \equiv (x_{i,t}, y_{i,t})$ and $x_{i,t}$ and $y_{i,t}$ are the coordinates of the i^{th} agent at time t . The locations may be observed for an m_t subset of the N agents, meaning all of the agents may not have location history for all T time points. In practice, this could result from a collar being enabled or disabled during the study period or the failure to record a location at that time. Similarly, the latent locations of the agents are denoted as $\mathbf{s}_t \equiv \{\mathbf{s}'_{1,t}, \dots, \mathbf{s}'_{N,t}\}$, where $\mathbf{s}_{i,t} \equiv (\tilde{x}_{i,t}, \tilde{y}_{i,t})$ and $\tilde{x}_{i,t}$ and $\tilde{y}_{i,t}$ are the latent coordinates of the i^{th} agent at time t . Then the observation equation is expressed as:

$$\mathbf{z}_t = \mathbf{H}_t \mathbf{s}_t + \boldsymbol{\epsilon}_t, \quad \boldsymbol{\epsilon}_t \sim N(\mathbf{0}, \sigma_\epsilon^2 I), \quad (1)$$

140 where \mathbf{H}_t is a $2m_t \times 2N$ incidence matrix of zeros and ones used to account for agents that
 141 are not observed at time t . The measurement error in the model is represented by σ_ϵ^2 ,
 142 which in this case incorporates uncertainty from both the GPS signal as well as impacts from

143 aligning the bear location fixes as measurements do not occur at precisely the same time.

144 **Evolution (State) Equation**

In the state-space literature, the terms state equation and evolution equation are used interchangeably. Here we use evolution equation to avoid confusion between the state equation and the behavior states of the switching model. The evolution equation for an individual agent, agent i in this case, is specified as

$$\underline{\mathbf{s}}_{\mathbf{i},t} \sim N(\underline{\mathbf{s}}_{\mathbf{i}-1,t} + u_{i,j,t}\underline{\delta}_{\mathbf{i},\mathbf{j},t}, \sigma_{\eta}^2 I), \quad (2)$$

145 where the term $u_{i,j,t}$ is a scalar variable representing agent i 's speed when in behavioral state j
146 at time t , $\underline{\delta}_{\mathbf{i},\mathbf{j},t} = (\delta_{x,i,j,t}, \delta_{y,i,j,t})$ is a unit vector describing the directional component of agent
147 i 's velocity when in state j at time t , and σ_{η}^2 is a random perturbation. The speed and angular
148 direction can be jointly estimated, or as is often the case, estimated separately. The speed
149 and angle parameters largely contribute to animal movement, but the direction of home range
150 and the presence of other individuals can also inform an agent's speed and angular heading.
151 In our particular setting speed is defined as the average distance between the location fixes
152 that are 12 hours apart, which can be different than the actual distance traveled by an
153 agent in that time window. Velocity combines the speed with an angular direction. We
154 chose 12-hr location fixes because the research question motivating this work is focused on
155 longer-term dynamics and range. Furthermore, centering the location fixes near crepuscular
156 hours reflects times when grizzly bears are most active, and thus most likely to interact.
157 Among grizzly bears, primary drivers of interactions are not necessarily direct, physical
158 encounters but involve indirect attracting and repulsive forces that manifest themselves at
159 coarse temporal and spatial scales. Such interactions are mediated, for example, through
160 scent communication or other cues that indicate the presence or density of conspecific bears.

The directional component of velocity is determined by an angle parameter $\theta_{i,j,t}$ such

that $(\delta_{x,i,j,t}, \delta_{y,i,j,t}) = (\cos(\theta_{i,j,t} + \nu_{i,j,t}), \sin(\theta_{i,j,t} + \nu_{i,j,t}))$ is modeled as

$$\theta_{i,j,t} \sim PN(\underline{\mu}_{\theta,j}, \Sigma_j), \quad (3)$$

161 where $PN()$ is a projected normal distribution, $\underline{\mu}_{\theta,j}$ is a mean vector, and Σ_j is a covariance
 162 matrix. The projected normal distribution transforms Cartesian coordinates to polar coor-
 163 dinates to acquire the angular values. The parameters in the projected normal distribution
 164 can be modeled as a function of other parameters, such as home range direction, location and
 165 turning angle of other agents, and/or behavioral state. The $\theta_{i,j,t}$ variable can be combined
 166 with another angle, $\nu_{i,j,t}$, that centers the direction and creates a biased random walk where
 167 agents tend to stay in the same home range or on a existing heading.

The speed model is specified as:

$$u_{i,j,t} \sim LN(\mu_{u,j}, \sigma_{u,j}^2) \quad (4)$$

168 where $LN()$ is a log normal distribution. Different frameworks can be used to model speed;
 169 however, a log normal distribution fits well with the data and also provides computational
 170 advantages of Gibbs samples inside the P-MCMC framework.

171 With a switching model, transition probabilities between the behavioral states also need
 172 to be specified. In this work, a two-state model is introduced, but the model framework
 173 is flexible and could permit multiple states. We use a predefined threshold where agents
 174 are aware of surrounding agents to induce different movement patterns. Based on biological
 175 understanding of grizzly bear's sphere of influence and uncertainty induced by using 12-hour
 176 location fixes, the threshold for our data analysis is set to 10 km. In situations where scientific
 177 understanding is not available to inform this distance, the threshold could be calibrated using
 178 predictive results or estimated by placing a prior distribution on this parameter. The two-
 179 state model requires estimating four probabilities $\underline{p} = (p_{12}[c], p_{12}[f], p_{22}[c], p_{12}[f])$, where $p_{i,j}$
 180 is the switching probability from state i from state j . The proximity of other agents are

181 specified in a binary framework using $[c]$ for close and $[f]$ for far away. Using conditionally
182 conjugate beta priors allows efficient samples from the posterior distributions.

Hierarchical structure can allow movement patterns to differ by agents within a population. For instance, building off the model for speed in Equation 4, rather than the same speed term for all agents, $\mu_{u,j}$, the speed term could be formulated in a hierarchical model so that each agent has a different speed term, $\mu_{u,i,j}$. This would result in speed parameters that can vary by agent:

$$\mu_{u,i,j} \sim N(\mu_{u,j}, \tau_j^2), \quad (5)$$

183 where $\mu_{u,j}$ would be the population level step length parameters, whereas $\mu_{u,i,j}$ could vary
184 by agent. Similarly, angle and transition probabilities can also be modeled in a hierarchical
185 framework.

186 To complete the Bayesian specification, prior distributions are needed for the following
187 parameters: σ_ϵ^2 , σ_η^2 , Σ_j , $\mu_{\theta,j}$, $\mu_{u,j}$, σ_u^2 , and \underline{p} . In general, conjugate and semi-conjugate
188 priors are used. Subject matter knowledge can be used to help inform hyperparameters
189 for the prior distributions. For instance, biological knowledge can be used for determining
190 reasonable distances a bear could travel in 12 hours. The appendix contains the complete
191 model formulation, including prior specification, for the data analysis of grizzly bears in the
192 GYE.

193 4 Computation

Fasiolo et al. (2016) outlines two common approaches for highly complex, nonlinear state-space models: ABC and P-MCMC. The extended Kalman filter has also been used in this setting (Orderud, 2005). The challenge in state-space models, such as this ABM formulation, is to jointly sample from the model parameters, denoted Θ , along with the state parameters, denoted \mathcal{X} . With the model specified in Section 3.1, there are a large number of state variables that need to be estimated. In particular, for each agent and time point, a step size

variable, turning angle variable, and a behavioral state parameter are required, which are combined with noise to result in two latent location parameters, a latitude and longitude. Thus, estimating the state parameters, which depend on Θ , requires jointly evaluating many state variables. Hence, exploring the space of the joint posterior distribution

$$p(\Theta, \mathcal{X}|\mathcal{Z}), \tag{6}$$

194 where \mathcal{Z} contains the observed locations of the agents, is difficult.

195 Approximate Bayesian Computation (ABC) is used for scenarios where evaluating the
 196 likelihood is difficult or impossible. Rather than directly evaluating the likelihood, a dataset
 197 is generated with the mechanistic model using a proposed value of the parameter set Θ . Then,
 198 a summary statistic, or set of summary statistics, are computed for the generated dataset.
 199 This summary statistic on the generated data is compared with a summary statistic on the
 200 observed data. If the distance between the summary statistics is sufficiently small, then
 201 the proposed value of Θ is accepted; otherwise, the proposed value is rejected. McDermott
 202 et al. (2017) presents a hybrid MCMC algorithm for jointly estimating additional model
 203 parameters along with the ABC approach for state parameters.

204 An alternative to ABC methods involves using P-MCMC where particle-based methods
 205 are used for MCMC proposals. One benefit of P-MCMC, versus ABC, is that the estimation
 206 is fully Bayesian, rather than approximate. As stated, the challenge with fitting this model is
 207 jointly estimating the model parameters and state variables in the joint posterior distribution,
 208 $p(\Theta, \mathcal{X}|\mathcal{Z})$. Using a standard Metropolis-Hasting approach for this model can be difficult,
 209 given the high dimensionality and correlation in the state variables. Particle MCMC uses
 210 particle filtering techniques, Sequential Monte Carlo (SMC), to propose $p(\mathcal{X}|\mathcal{Z}, \Theta)$. In other
 211 words, given the parameter values, Θ , a particle filter is used to propose a set of state values.

212 The common criticism of SMC techniques is that the methods suffer from particle de-
 213 generacy as the number of distinct samples becomes small enough that the estimates of the

214 joint likelihood are unreliable. This issue is exacerbated as the total number of time points
 215 becomes larger and model fitting requires a, perhaps unfeasible, large number of particles.
 216 The problem is lessened in P-MCMC as Andrieu et al. (2010) state “PMCMC sampling is
 217 much more robust and less likely to suffer from this depletion problem. This stems from the
 218 fact that PMCMC algorithms do not require SMC algorithms to provide a reliable approxi-
 219 mation of [the sampling distribution of the state variables], but only to return a single sample
 220 approximately distributed according to [sampling distribution of the state variables].” With
 221 that said, with the P-MCMC algorithm we opted to use the Particle Marginal Metropolis-
 222 Hastings approach rather than the Particle Gibbs approach as we found better mixing of the
 223 state parameters. Additionally, a much longer time series, such as using hourly data rather
 224 twice-daily location fixes and/or a large increase in the number of agents, would certainly
 225 tax the algorithm.

226 **P-MCMC Algorithm**

227 Let Θ be a set of model parameters, which in this case have closed form full conditional
 228 distributions. An overview of a basic P-MCMC algorithm can be seen in Algorithm 1.

229

```

for  $iter = 1$  to  $M$  do
  |
  | 1. Sample  $\Theta|-$  from full conditional distributions ;
  | 2. Propose  $\mathcal{X}^*$  using particle filter conditional on  $\Theta^{(iter)}$  ;
  | 3. Accept  $\mathcal{X}^*$  according to  $p(\mathcal{X}|\mathcal{Z}, \Theta^{(iter)})$  with the standard Metropolis-Hastings
  |    acceptance ratio
end

```

230

Algorithm 1: Basic P-MCMC Algorithm (Particle Marginal Metropolis-Hastings)

231

232 A detailed algorithm for the models shown in Section 3.2 can be found in the appendix and
 233 computer code is provided in the supplemental materials section. A rather obvious drawback
 234 of P-MCMC is computing time, as each iteration of an MCMC algorithm requires a particle

235 filter with a large number of particles.

236 In all scenarios with weakly informative prior specification, the P-MCMC approach is
237 considerably easier to tune than ABC, in that it does not require as many researcher choices.
238 In particular, ABC requires the researcher to choose: 1.) a summary statistic, 2.) a distance
239 metric, and 3.) a kernel associated with that distance between the observed and simulated
240 data. While P-MCMC model fit is based on the statistical likelihood, ABC can be calibrated
241 on metrics that are not part of the likelihood, such as some summary of collective movement.
242 Complicating factors for ABC include that the summary statistics are typically application
243 dependent, and even in the simulation studies conducted in this article, where the true
244 behavior parameters are known, it is challenging to calibrate the algorithm to return accurate
245 results. In contrast, the only parameter to tune in the P-MCMC framework is the number
246 of particles, which controls the acceptance rate of the Metropolis proposal for the state
247 parameters. The trade off is that P-MCMC approach requires fitting a SMC algorithm
248 with a large number of particles for every iteration of the MCMC sampler, which presents a
249 computational burden.

250 Given the computational requirements of the P-MCMC approach, the algorithms are
251 implemented in the programming language Julia (Bezanson et al., 2017). Julia has been
252 shown to execute similar programs several orders of magnitude quicker than R and results
253 in a substantial reduction in the analysis time. In our experience and with our coding, the
254 particle filter component of the model is roughly an order of 50 - 100 times faster in Julia
255 than in R.

256 **5 Model Demonstration**

257 **5.1 Synthetic Data Analysis**

258 With this section we simulate data similar to the grizzly bear data to determine the efficacy
259 of estimating the model switching parameters and making predictions of future locations.

260 In particular, we simulate synthetic bear data from the models in Equations 1 - 6 and then
261 evaluate the ability of P-MCMC to recover model parameters and predict future movement.
262 Finally the predictive capacity of models with and without collective behavior are compared.

263 Typically a manuscript makes comparisons between a proposed method and the best
264 existing alternatives. In this case, existing agent-based collective movement models have been
265 primarily designed for animals with herding or schooling behaviors, neither which would be
266 applicable to grizzly bears. McDermott et al. (2017) present a general approach for collective
267 animal movement, but, as previously discussed, the ABC approach presents difficulties in
268 choosing summary statistics, kernels, and tuning. Hence, the logical comparison is with a
269 model that does not implement any collective movement characteristics, that is one that uses
270 the principles of correlated random walks, but does not consider locations of other animals.

271 Four different simulation scenarios are conducted: the collective movement signal varies
272 across the first three simulations and the fourth has no collective movement. Weakly infor-
273 mative, conjugate priors are used in both simulations. Complete specification and Julia code
274 for re-creating the synthetic data analyses are available in the supplemental materials. For
275 each scenario, 90 time points for 30 synthetic bears are simulated. Another 120 time points
276 are reserved for predictive comparisons. Each simulation setting is replicated twenty different
277 times. For simulation 1, the switching behavior is largely influenced by proximity of other
278 agents and the movement patterns are well separated between the two states. For simulation
279 2 and simulation 3, the switching behavior as a function of agent proximity becomes less
280 pronounced. Similarly, for simulation 2 and simulation 3, the movement patterns become
281 progressively less separated between the two states. For simulation 4, there is no collective
282 movement in the simulated data. The parameters used to generate the movement data can
283 be seen in Figure 4. Across these four simulated scenarios, we compare the ability of the two
284 model specifications to estimate the model parameters, with special attention given to the
285 model switching behavior, and also compute the accuracy of k-step ahead predictions.

286 **5.1.1 Parameter Estimation**

287 Simulated paths for simulation 2, which has a moderate collective movement signal, are
shown in Figure 3. The shape icon denotes whether or not the agent is in the exploratory



Figure 3: A sample of simulated bear paths (top). Close up look at simulated paths of bear id 3 (bottom), which is shown in purple. State two, the triangles, corresponds to exploring.

288

289 behavioral pattern and the lines are estimated paths. These synthetic data are from one

290 realization of simulation 2. From this figure, the inertia of the synthetic bears is apparent,
291 as the bears tend to stay either in state one or state two. What isn't as obvious, without
292 the benefit of animation, is that when bears are in proximity it tends to result in transitions
293 to state 2, with larger steps and similar heading to previous steps.

294 The true parameters as well as estimates from the simulation realizations can be seen in
295 Figure 4. In general, the parameters are similar for the two models and match the values
296 from the simulated data. Both modeling frameworks also tend to identify the states fairly
297 accurately. However, the notable exception is the switching probabilities. In the three
298 simulation scenarios with collective movement, the independent movement model does a
299 poor job of estimating the switching probabilities. This is not surprising as there is not a
300 mechanism in those models to switch states based on other agents in the area.

301 Without a mechanism for accounting for collective movement, or the proximity of other
302 agents, the independent model does not capture the switching probability when agents are
303 inside a threshold that causes behavioral changes. The proportion of time points where
304 the agents are close together is fairly small, but these events are important drivers of land
305 use. Furthermore, the predictive densities, when agents are close together, can be greatly
306 influenced by failing to account for agent proximity and differing behaviors. Figure 5 con-
307 tains an illustrative example, using the estimated parameters from simulation 3, where the
308 independent model fails to account for the proximity of the nearest agent.

309 **5.1.2 Predictive Densities**

310 To evaluate the k-step ahead prediction we use the mean absolute deviation (MAD) between
311 the observed locations and the mean of the posterior predictions. The expected difference
312 in MAD between a collective movement model and the independent model can be seen in
313 Figure 6. The expected difference in MAD is calculated using the twenty replicates for
314 each simulation setting. In all three collective movement scenarios, simulations 1, 2, and
315 3, the collective movement model contains a predictive advantage. For simulation 1, where

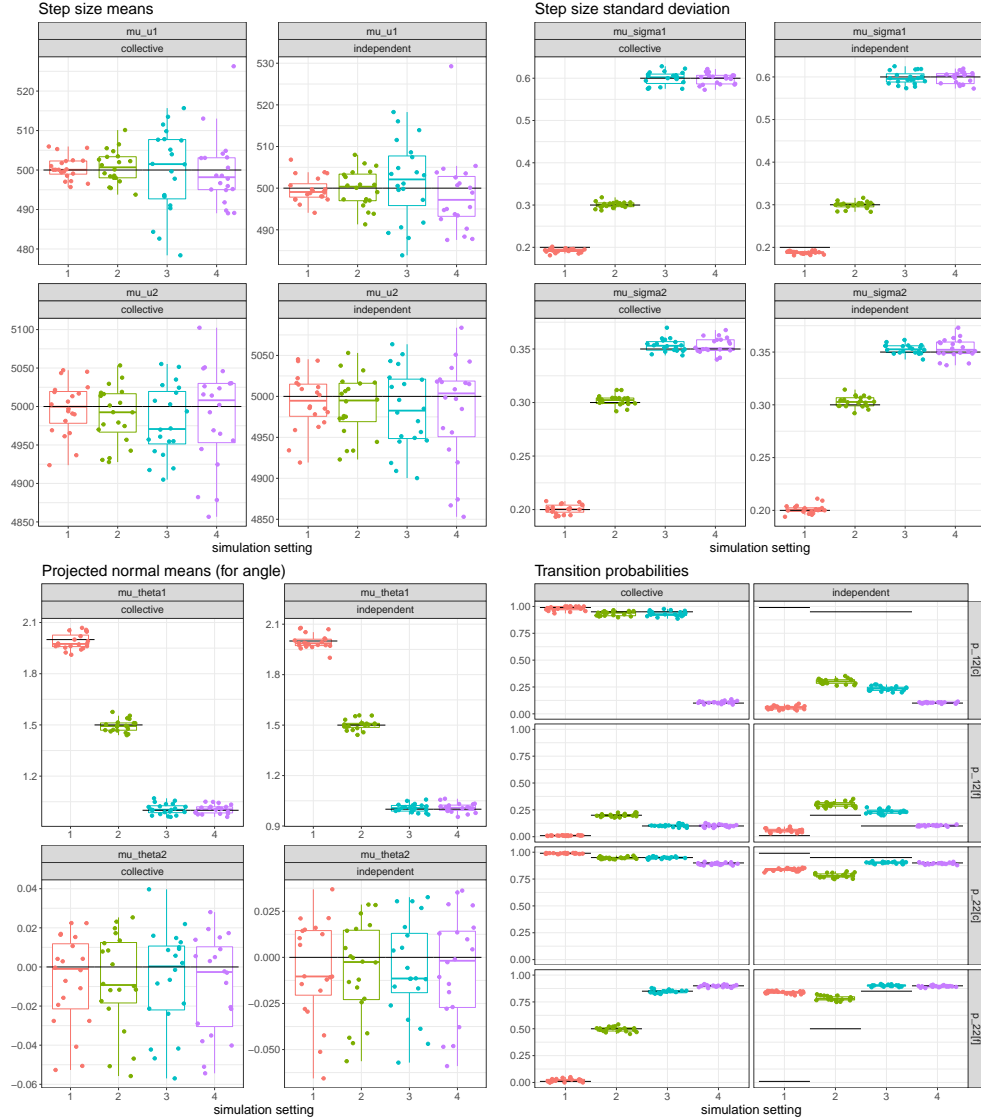


Figure 4: Known parameters from the simulation (black bars) and simulated results for a set of twenty simulated realizations are shown. The step size means, step size standard deviations, and angle parameters are estimated fairly precisely for both the collective movement and independent movement models. The key difference is the independent model’s inability to estimate different behaviors when other agents are in close proximity. The top panel of the bottom right figure corresponds to the probability of switching to an exploring state when other agents are close by.

316 the collective movement signal is strong and the synthetic bears tend to stay in the same
 317 state for longer periods, the prediction improvement continues to grow as k increases. For
 318 simulations 2 and 3, which have more moderate, and likely realistic, collective movement, the



Figure 5: This figure demonstrates the model switching behavior in the collective movement model. The proximity of an other agent, denoted with a triangle, switches the exploratory behavior for the collective movement model, whereas, the independent movement model stays largely in the home range state.

319 prediction increases level out, or increase minimally, after the first few time periods. Finally,
 320 in the final scenario with no collective movement, there are no discernible differences in the
 321 predictive results between the collective movement and independent models.

322 For the first three simulation settings, the predictive difference is magnified when syn-
 323 thetic bears are in close proximity to other individuals. The difference in MAD between
 324 collective movement models and independent models is larger, for the first step or two,
 325 than the average across all synthetic bears that is displayed in Figure 6. A demonstration of
 326 the differences between the two models, when other bears are in close proximity, can be seen
 327 in Figure 5, which shows a set of predicted paths for an agent that has another agent in close
 328 proximity. Using the estimated parameters from the model, the collective movement model
 329 would largely result in a state switch to the exploratory state, whereas, with the independent
 330 model bears would tend to stay in the home-range state.

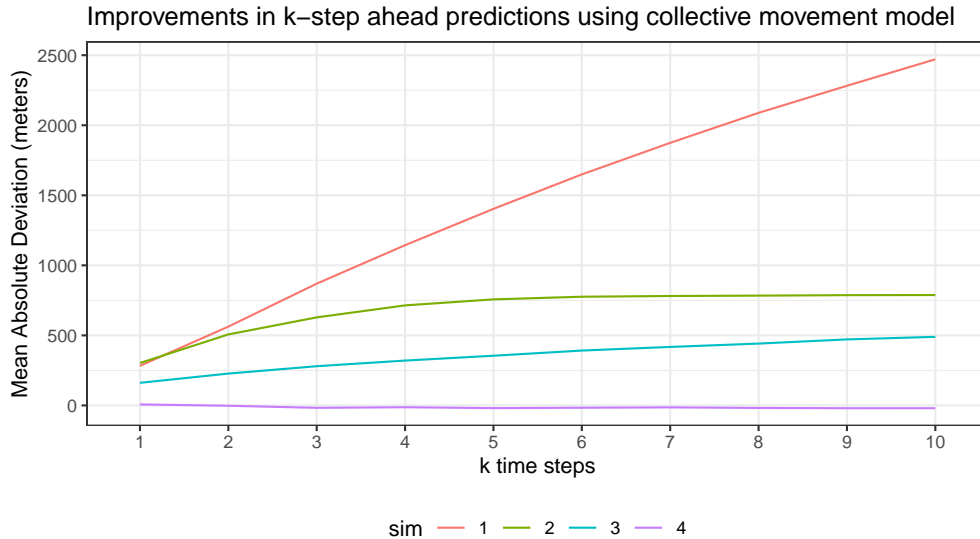


Figure 6: The expected improvement in Mean Absolute Deviation (MAD) for a collective movement model relative to the independent model is shown. With the three collective movement settings (simulations 1 - 3), there is a predictive improvement, but the improvement is lessened as the collective movement model becomes weaker. With no collective movement, in simulation 4, there is not a discernible difference between the two approaches.

331 5.1.3 Summary

332 For the simulation settings when collective movement exists in the data, the collective move-
 333 ment model improved parameter estimation and predictive performance. In simulation 4,
 334 when no collective movement exists, there are little differences between the two models.
 335 When collective movement does occur, the collective movement model is superior. When
 336 collective movement is not present, the model does not do appreciably worse.

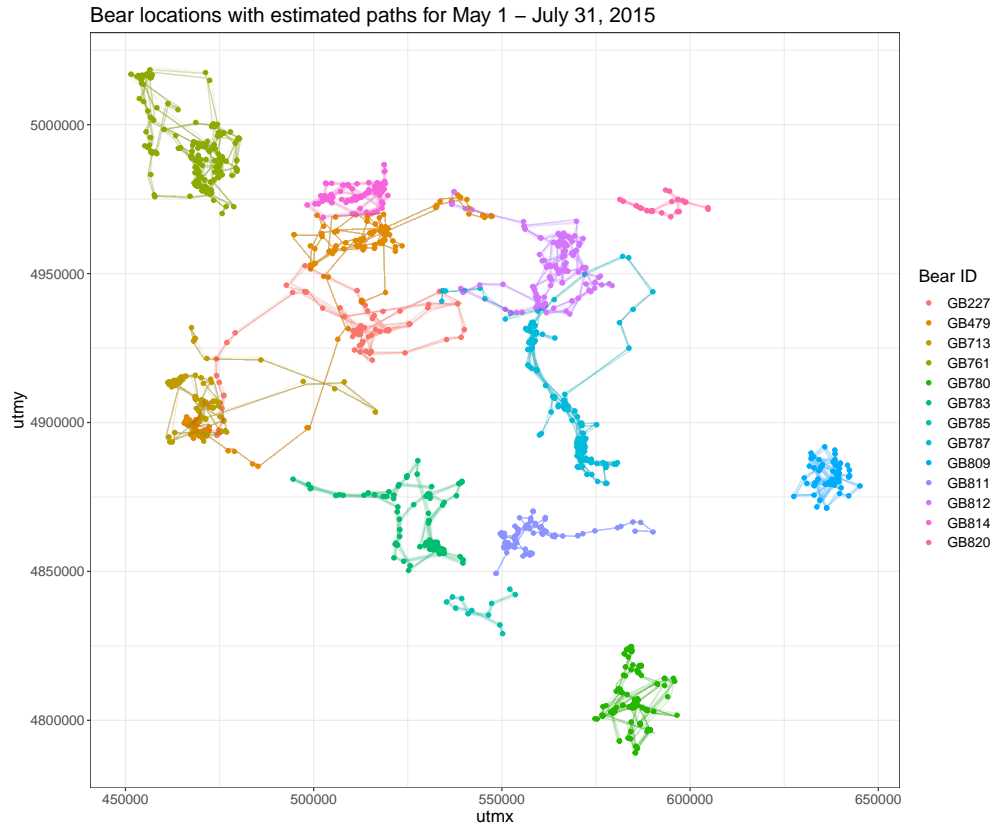
337 5.2 Application: Grizzly Bear Movement

338 The collective movement model is applied to the grizzly bear data described in Section 2.
 339 With this model, we find bears spend 47.1 (46.5, 47.5) percent of their time in the state with
 340 shorter steps oriented toward a moving average of previous positions and the remaining 52.9
 341 (52.5, 53.5) percent of the time in the state with longer steps oriented on the same heading.
 342 While the movement types may suggest associated behavior states, such as "home range" and

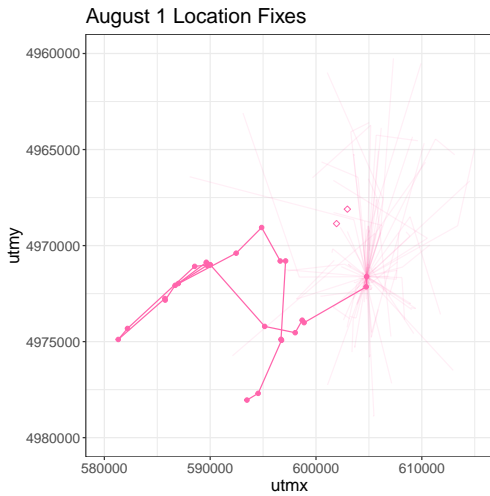
343 "exploring," that correspond to the states of the model, but without labeled observational
344 data the suggested behavioral states do not necessarily have a one-to-one correspondence
345 with the movement patterns. The posterior means for the step size parameters for the
346 lognormal distribution are $\mu_u = 5.78$ (5.70, 5.86) and $\sigma_u = 1.06$ (1.02, 1.10) for the "home
347 range" state and $\mu_u = 8.29$ (8.27, 8.31) and $\sigma_u = 0.72$ (0.70, 0.74) for the "exploring" state,
348 which results in median step size of around 300 and 4000 meters, respectively. We note we
349 use the term "exploring" in a broad biological sense of movements influenced by the presence
350 of other bears while remaining within their respective home ranges. The parameters for
351 the projected normal distribution, which correspond to the angular heading are estimated
352 as 0.56 (0.52, 0.59) and -0.05 (-0.09, 0.02). This suggests, unsurprisingly, that the angular
353 heading of the bears is more uncertain than in the simulation setting.

354 The bears tend to switch states at a higher rate than the simulated datasets. Furthermore,
355 there is evidence that switching behavior does change when in the proximity of other bears.
356 The switching probabilities are $p_{12[f]} = 0.32$ (0.31, 0.34), $p_{12[c]} = 0.39$ (0.35, 0.43), $p_{22[f]} =$
357 0.72 (0.70, 0.73), and $p_{22[c]} = 0.68$ (0.60, 0.69). In particular, a bear in "home range" state
358 is more likely to switch to "exploring" when in the proximity of other bears. The credible
359 intervals associated with the switching probabilities provide evidence in favor of using the
360 collective movement model in this situation.

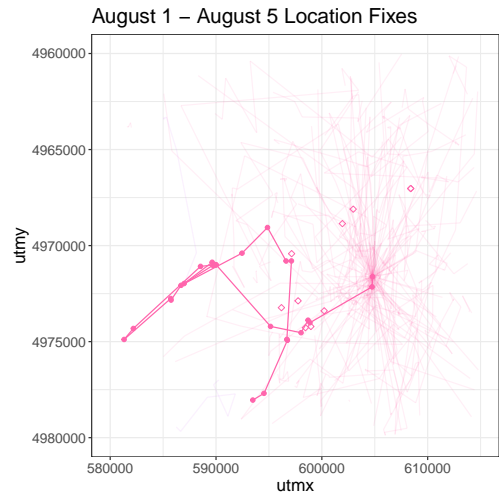
361 Given the motivation of this work is to understand longer-term grizzly bear land use
362 patterns, we use the holdout data from August to evaluate prediction of future locations.
363 With this framework, the question of interest is not focused on where will the bear be located
364 on step $t+k$, but rather the focus is on all the locations that a bear could visit between time t
365 and $t+k$. Figure 7 shows recorded locations and estimated paths for the period of May - July
366 in 2015. The figure also contains an up-close view of predicted paths for 1 day (2-steps) and
367 5 days (10-steps) for bear GB820. From a practical purpose, these k-step ahead predictions
368 from this model can also be used to calibrate changes in space use. Predictions for the first
369 week have a mean absolute deviation of 9800 meters (and a median absolute deviation of



(a) The points represent recorded locations and lines correspond to the estimated paths.



(b) Predicted paths for August 1.



(c) Predicted paths for August 1 - August 5.

Figure 7: The top figure contains observed location fixes and estimated paths for all bears from May 1 - July 31 in 2015. The bottom two figures contain observed location and predicted paths for GB820 for 2-step ahead predictions on August 1 (left) and 10-step ahead predictions for August 1 - August 5 (right). The diamonds represent the actual 2 or 10-step ahead predictions.

370 6600 meters). Extending the predictions to the entire month, the mean absolute deviation is
371 about 14,600 meters, while the median absolute deviation is just more than 10,000 meters.

372 **6 Discussion**

373 For many species the movement patterns of an individual depend upon the collective locations
374 of other individuals. Existing research in collective movement models has largely focused on
375 species that exhibit herding or schooling behavior. With this article, we present an ABM,
376 along with fully Bayesian parameter estimation, designed for species in which both attractive
377 or repulsive effects of conspecific animals can influence movement dynamics. In particular,
378 our model is developed with a focus on grizzly bears, but it could be widely applicable to
379 other species with common behaviors.

380 Our synthetic data analysis suggests that using a model designed to capture collective
381 movement does not result in adverse predictions, when collective movement does not exist,
382 however, it results in improved performance relative to a model that does not consider
383 locations of other individuals. Using this model with twice-daily grizzly bear locations, there
384 is evidence of different behavioral patterns in the presence of other bears.

385 The model also provides a mechanism for predicting future movement patterns. Using
386 holdout data, median absolute prediction error for the next week is roughly 6600 meters and
387 the median absolute deviation prediction error for the next month is just more than 10,000
388 meters. The model provides a framework that enables predictive paths for k-steps ahead,
389 which can be used, for example, to estimate future occupied range, a critical information need
390 for wildlife managers. To predict expansion of future occupied range, future research will
391 focus on collective movement patterns and dispersal dynamics in combination with habitat
392 and terrain attributes.

Acknowledgements

We thank the member agencies of the Interagency Grizzly Bear Study Team for data contributions: U.S. Geological Survey, National Park Service; U.S. Fish and Wildlife Service; U.S. Forest Service; Wyoming Game and Fish Department; Montana Fish, Wildlife and Parks; Idaho Department of Fish and Game; and the Eastern Shoshone and Northern Arapaho Tribal Fish and Game Department. We thank Joseph D. Clark for his review as part of the U.S. Geological Survey’s Fundamental Science Practices. Any use of trade, firm, or product names is for descriptive purposes only and does not imply endorsement by the U.S. Government.

We also thank Stephen Walsh for the motivation to try Julia and the patience for answering our questions.

References

- Andrieu, C., Doucet, A., and Holenstein, R. (2010). Particle Markov chain Monte Carlo methods. *Journal of the Royal Statistical Society: Series B (Statistical Methodology)*, 72(3):269–342.
- Ballerini, M., Cabibbo, N., Candelier, R., Cavagna, A., Cisbani, E., Giardina, I., Orlandi, A., Parisi, G., Procaccini, A., Viale, M., et al. (2008). Empirical investigation of starling flocks: a benchmark study in collective animal behaviour. *Animal behaviour*, 76(1):201–215.
- Beaumont, M. A. (2010). Approximate Bayesian computation in evolution and ecology. *Annual review of ecology, evolution, and systematics*, 41:379–406.
- Beaumont, M. A., Zhang, W., and Balding, D. J. (2002). Approximate Bayesian computation in population genetics. *Genetics*, 162(4):2025–2035.
- Bezanson, J., Edelman, A., Karpinski, S., and Shah, V. B. (2017). Julia: A fresh approach to numerical computing. *SIAM review*, 59(1):65–98.

- 417 Bonnell, T. R., Henzi, S. P., and Barrett, L. (2016). Direction matching for sparse movement
418 data sets: determining interaction rules in social groups. *Behavioral Ecology*.
- 419 Brown, D. G., Riolo, R., Robinson, D. T., North, M., and Rand, W. (2005). Spatial pro-
420 cess and data models: Toward integration of agent-based models and GIS. *Journal of*
421 *Geographical Systems*, 7(1):25–47.
- 422 Christ, A., Ver Hoef, J., and Zimmerman, D. L. (2008). An animal movement model in-
423 corporating home range and habitat selection. *Environmental and Ecological Statistics*,
424 15(1):27–38.
- 425 Couzin, I. D., Krause, J., Franks, N. R., and Levin, S. A. (2005). Effective leadership and
426 decision-making in animal groups on the move. *Nature*, 433(7025):513–516.
- 427 Couzin, I. D., Krause, J., James, R., Ruxton, G. D., and Franks, N. R. (2002). Collective
428 memory and spatial sorting in animal groups. *Journal of theoretical biology*, 218(1):1–12.
- 429 Ebinger, M. R., Haroldson, M. A., van Manen, F. T., Costello, C. M., Bjornlie, D. D.,
430 Thompson, D. J., Gunther, K. A., Fortin, J. K., Teisberg, J. E., Pils, S. R., et al. (2016).
431 Detecting grizzly bear use of ungulate carcasses using global positioning system telemetry
432 and activity data. *Oecologia*, 181(3):695–708.
- 433 Farmer, J. D. and Foley, D. (2009). The economy needs agent-based modelling. *Nature*,
434 460(7256):685.
- 435 Fasiolo, M., Pya, N., Wood, S. N., et al. (2016). A comparison of inferential methods
436 for highly nonlinear state space models in ecology and epidemiology. *Statistical Science*,
437 31(1):96–118.
- 438 Gilbert, N. (2008). *Agent-based models*. Sage.
- 439 Gilbert, N. and Terna, P. (2000). How to build and use agent-based models in social science.
440 *Mind & Society*, 1(1):57–72.

- 441 Haydon, D. T., Morales, J. M., Yott, A., Jenkins, D. A., Rosatte, R., and Fryxell, J. M.
442 (2008). Socially informed random walks: incorporating group dynamics into models of
443 population spread and growth. *Proceedings of the Royal Society of London B: Biological*
444 *Sciences*, 275(1638):1101–1109.
- 445 Hooten, M. B., Johnson, D. S., McClintock, B. T., and Morales, J. M. (2017). *Animal*
446 *movement: statistical models for telemetry data*. CRC press.
- 447 Hooten, M. B. and Wikle, C. K. (2010). Statistical agent-based models for discrete spatio-
448 temporal systems. *Journal of the American Statistical Association*, 105(489):236–248.
- 449 Jonsen, I. D., Flemming, J. M., and Myers, R. A. (2005). Robust state–space modeling of
450 animal movement data. *Ecology*, 86(11):2874–2880.
- 451 Kahle, D. and Wickham, H. (2013). ggmap: Spatial visualization with ggplot2. *The R*
452 *Journal*, 5(1):144–161.
- 453 Langrock, R., Hopcraft, J. G. C., Blackwell, P. G., Goodall, V., King, R., Niu, M., Patterson,
454 T. A., Pedersen, M. W., Skarin, A., and Schick, R. S. (2014). Modelling group dynamic
455 animal movement. *Methods in Ecology and Evolution*, 5(2):190–199.
- 456 Langrock, R., King, R., Matthiopoulos, J., Thomas, L., Fortin, D., and Morales, J. M.
457 (2012). Flexible and practical modeling of animal telemetry data: hidden Markov models
458 and extensions. *Ecology*, 93(11):2336–2342.
- 459 McClintock, B. T., King, R., Thomas, L., Matthiopoulos, J., McConnell, B. J., and Morales,
460 J. M. (2012). A general discrete-time modeling framework for animal movement using
461 multistate random walks. *Ecological Monographs*, 82(3):335–349.
- 462 McDermott, P. L., Wikle, C. K., and Millsbaugh, J. (2017). Hierarchical nonlinear spatio-
463 temporal agent-based models for collective animal movement. *Journal of Agricultural,*
464 *Biological and Environmental Statistics*, 22(3):294–312.

- 465 Morales, J. M., Haydon, D. T., Frair, J., Holsinger, K. E., and Fryxell, J. M. (2004). Ex-
466 tracting more out of relocation data: building movement models as mixtures of random
467 walks. *Ecology*, 85(9):2436–2445.
- 468 Nuñez-Antonio, G., Ausín, M. C., and Wiper, M. P. (2015). Bayesian nonparametric models
469 of circular variables based on Dirichlet process mixtures of normal distributions. *Journal*
470 *of Agricultural, Biological, and Environmental Statistics*, 20(1):47–64.
- 471 Orderud, F. (2005). Comparison of kalman filter estimation approaches for state space
472 models with nonlinear measurements. In *Proc. of Scandinavian Conference on Simulation*
473 *and Modeling*, pages 1–8. Citeseer.
- 474 Peck, C. P., van Manen, F. T., Costello, C. M., Haroldson, M. A., Landenburger, L. A.,
475 Roberts, L. L., Bjornlie, D. D., and Mace, R. D. (2017). Potential paths for male-mediated
476 gene flow to and from an isolated grizzly bear population. *Ecosphere*, 8(10):e01969.
- 477 Pedersen, T. L. (2019). *ggforce: Accelerating 'ggplot2'*. R package version 0.3.1.
- 478 Ritter, C. and Tanner, M. A. (1992). Facilitating the Gibbs sampler: the Gibbs stopper and
479 the griddy-Gibbs sampler. *Journal of the American Statistical Association*, 87(419):861–
480 868.
- 481 Scharf, H. (2019). *anipaths: Animation of Observed Trajectories Using Spline-Based Inter-*
482 *polation*. R package version 0.9.7.
- 483 Scharf, H. R., Hooten, M. B., Wilson, R. R., Durner, G. M., and Atwood, T. C. (2019).
484 Accounting for phenology in the analysis of animal movement. *Biometrics*.
- 485 Vicsek, T., Czirók, A., Ben-Jacob, E., Cohen, I., and Shochet, O. (1995). Novel type of
486 phase transition in a system of self-driven particles. *Physical review letters*, 75(6):1226.
- 487 Wang, F. and Gelfand, A. E. (2013). Directional data analysis under the general projected
488 normal distribution. *Statistical methodology*, 10(1):113–127.

489 Wickham, H. (2016). *ggplot2: Elegant Graphics for Data Analysis*. Springer-Verlag New
490 York.

491 Appendix

492 P-MCMC Algorithm

493 Using conjugate priors, the sampling largely consists of Gibbs steps along with a particle
494 approach for the state parameters.

- 495 1. Propose new set of state parameters using marginal particle proposal. Specifically,
496 a particle filter is used to propose \mathcal{S} , \mathcal{X} , δ , and *state* conditional on the remaining
497 parameters in the model. The script notation refers to all of the variables of that
498 type, across agents, years, and time points. Proposals are accepted with the typical
499 Metropolis-Hastings ratio as detailed in Andrieu et al. (2010). This procedure updates
500 one agent at a time, within a given year, but the procedure can be parallelized across
501 years.
- 502 2. The probability parameters associated with the state transitions are fit using conjugate
503 priors from a beta distribution.
- 504 3. The step size ($\mu_{u,j}$) and variance parameters ($\sigma_{u,j}^2$) in the lognormal distribution for
505 each state can be sampled using a Gibbs sampler.
- 506 4. The variance associated with the measurement error (σ_ϵ) can be sampled from an
507 inverse gamma distribution.
- 508 5. The final piece is taking samples from the projected normal, Nuñez-Antonio et al.
509 (2015) outlines a Griddy-Gibbs approach (Ritter and Tanner, 1992) for this procedure.
510 With this approach, the angular data (θ) is converted to Cartesian coordinates, where
511 $x = r \cos(\theta)$ and $y = r \sin(\theta)$. Integrating out r and using the x and y data enables
512 Gibbs samples for the mean of the projected normal. Wang and Gelfand (2013) presents
513 a more general approach for sampling from a projected normal distribution.

514 6.1 Model Specification and Priors for Data Analysis

515 Observation Equation

$$\mathbf{z}_t \sim N(\mathbf{H}_t \mathbf{s}_t + \boldsymbol{\varepsilon}_t, \sigma_\varepsilon^2 I)$$

516 Evolution Equation

$$\mathbf{s}_{i,t} = \mathbf{s}_{i-1,t} + u_{i,j,t} \delta_{i,j,t}$$

$$\delta_{i,j,t} = (\cos(\theta_{i,j,t} + \nu_{i,j,t}), \sin(\theta_{i,j,t} + \nu_{i,j,t}))$$

$$\theta_{i,j,t} \sim PN(\underline{\mu}_{\theta,j}, I)$$

$$u_{i,j,t} \sim LN(\mu_{u,j}, \sigma_{u,j}^2)$$

$$p_{12[c]} = Pr[j_t = 1 \rightarrow j_{t+1} = 2 | d_t < thr]$$

$$p_{12[f]} = Pr[j_t = 1 \rightarrow j_{t+1} = 2 | d_t > thr]$$

$$p_{22[c]} = Pr[j_t = 2 \rightarrow j_{t+1} = 2 | d_t < thr]$$

$$p_{22[f]} = Pr[j_t = 2 \rightarrow j_{t+1} = 2 | d_t > thr],$$

517 where $j = 1$ is the model state with shorter steps that tend to stay in the same area,
 518 $j = 2$ is the model state with larger steps that tend to maintain the existing heading, $\theta_{i,j,t}$
 519 is the stochastic component of the heading, where $\nu_{i,j,t}$ aligns the heading to a collection of
 520 previous locations for state i or the most recent heading for state j . The switching component
 521 of the model is determined by whether the distance to the nearest animal, d_t , is less than a
 522 threshold, thr .

523 **Prior Distributions**

In general, the prior distributions are weakly informative and aligned with biological understanding.

$$\sigma_\epsilon^2 \sim IG(5, 50000)$$

The prior for σ_ϵ^2 has a mean that roughly corresponds to a standard deviation of 100 meters.

$$\mu_\theta \sim N(\underline{(1, 0)^T}, .1I)$$

524 The prior for μ_θ is centered at $\underline{(1, 0)^T}$, with relatively weak precision, has little impact on
525 the posterior.

$$\mu_{u1} \sim N(\log(500), .5)$$

$$\mu_{u2} \sim N(\log(5000), .5)$$

$$\sigma_{u1}^2 \sim IG(5, 1.8)$$

$$\sigma_{u2}^2 \sim IG(5, 0.6)$$

526 The mean step size parameters are centered at 500 meters and 5000 meters (after ac-
527 counting for lognormal parameterization), but have small enough precision that they can be
528 largely informed by the data. Similarly, the standard deviation values are not particularly
529 influential.

$$p_{12[c]} \sim \text{Beta}(1.9, .1)$$

$$p_{12[f]} \sim \text{Beta}(.1, 1.9)$$

$$p_{22[c]} \sim \text{Beta}(1.9, .1)$$

$$p_{22[f]} \sim \text{Beta}(1.9, .1)$$

530 The priors for the transition probabilities suggest inertia (95 percent probability of staying
531 in same state), except for when another bear is in close proximity and a bear is in state 1, then
532 the prior probability of switching is 95 percent. However, the prior probabilities correspond
533 to 2 data points, so there is little impact on the posterior probability.